NUMERICAL STUDY OF TWO DIFFERENT TYPES OF SEMI-SUBMERSIBLE PLATFORMS WITH MOORING SYSTEMS IN THE SEA

Yao Peng, Decheng Wan*
State Key Laboratory of Ocean Engineering, School of Naval Architecture, Ocean and Civil Engineering, Shanghai Jiao Tong University, Collaborative Innovation Center for Advanced Ship and Deep-Sea Exploration, Shanghai 200240, China
*Corresponding author: dcwan@sjtu.edu.cn

ABSTRACT:
With the increasing demand of floating structures in ocean, various types of platforms and mooring systems are designed to meet the need. And it is of great significance for us to further understand how the platforms work with their mooring systems in different sea conditions. In this paper, motion responses of two different types of semi-submersible platforms with corresponding mooring systems are studied numerically by a viscous flow solver named naoe-FOAM-SJTU, which is developed from the open source toolbox OpenFOAM. One of the semi-submersible platforms is designed for the exploration and production of oil (named platform 1), and the other (named platform 2) is designed for the accommodation of works. Waves of different period are generated to study how the wave period influent the motion response of platform 1. We pay close attention to the motion responses of platforms and the forces in corresponding mooring lines. Several important conclusions are drawn.

INTRODUCTION

Semi-submersible platforms are commonly used for the exploration of deep-water oil. Generally, a semi-submersible platform suffers the loads of water and wind at sea. And in order to make sure that the semi-submersible platform work smoothly, mooring system are commonly used on the semi-submersible platform to resist the motion responses induced by environmental loads. As we can see, it's of great significance to investigate the mooring systems, especially their interaction with the semi-submersible platforms.

A lot of research has been done on how the mooring systems interact with floating structures such as a semi-submersible platform. Tahar and Kim [1] developed a time domain coupled analysis tool to study a floating platform with a mooring system. They adopted rod theory and finite element method to solve mooring lines. Kim, et al. [2] compared the dynamic coupled behaviour of moored floating structures in time domain. Sethurman and Venugopal [3] conduct a series of experiments for a floating stepped-spar wind turbine, and their result indicates that an accurate modeling of mooring line dynamics must consider the structure non-linearity and damping. Yilmaz [4] developed a time domain numerical model to predict the dynamic response of a semi-submersible platform. And they used their time domain simulations to find the total extreme motions and mooring forces of semi-submersibles. Carlos, et al. [5] took part in the AZIMUT project, they used the model the this project to study the estimation of the wave drift components and their effects on the design of the mooring system.

In this paper, two different shapes of semi-submersible platforms are studied. Platform 1 is built for the exploration and production of oil, and platform 2 is built for the accommodation

of workers. 8 mooring lines are adopted for both platforms, and parameters of the mooring systems are then presented. Wave period of 6s and 5s are adopted for the study of platform 1. A solver named naoe-FOAM-SJTU is adopted for the numerical simulation. Solver naoe-FOAM-SJTU is based on a built-in solver in OpenFOAM named interDyMFoam, which can be used to solve two incompressible, isothermal immiscible fluids with dynamic mesh motion. A six-degrees-of-freedom module and a mooring system module are developed and integrated into the naoe-FOAM-SJTU to better simulate the fluid-structure with mooring system. Study in this paper gives information to the designers for the primary prediction of motion response of the platforms.

NUMERICAL METHODS

Governing equations

For transient, incompressible and viscous fluid, flow problems are governed by Navier-Stokes equations:

$$\nabla \cdot \mathbf{U} = 0 \tag{1}$$

$$\frac{\partial \rho \mathbf{U}}{\partial t} + \nabla \cdot (\rho(\mathbf{U} - \mathbf{U}_g)\mathbf{U}) = -\nabla p_d - \mathbf{g} \cdot \mathbf{x} \nabla \rho + \nabla \cdot (\mu \nabla \mathbf{U}) + \mathbf{f}_\sigma \tag{2}$$

where U and U_g represent velocity of flow field and grid nodes separately; $p_d = p - \rho \boldsymbol{g} \cdot \boldsymbol{x}$ is dynamic pressure of flow field by subtracting the hydrostatic part from total pressure p; **g**, ρ and μ denote the gravity acceleration vector, density and dynamic viscosity of fluid respectively; f_σ is surface tension which only takes effect at the free surface and equals zero elsewhere.

Capture of free surface

Volume of Fluid (VOF) [6] method is adopted in naoe-FOAM-SJTU to capture free surface. The VOF transport equation is formulated as Eq.3.

$$\frac{\partial \alpha}{\partial t} + \nabla \cdot [(\mathbf{U} - \mathbf{U}_g)\alpha] + \nabla \cdot [\mathbf{U}_r(1-\alpha)\alpha] = 0 \tag{3}$$

Where α is the volume of fraction, representing the ratio of volume fluid occupies. And α can be defined as Eq.4.

$$\begin{cases} \alpha = 0, & air \\ \alpha = 1, & water \\ 0 < \alpha < 1, & free\ surface \end{cases} \tag{4}$$

The fluid density ρ and dynamic viscosity μ are obtained by Eq.5.

$$\begin{cases} \rho = \alpha \rho_l + (1-\alpha)\rho_g \\ \mu = \alpha \mu_l + (1-\alpha)\mu_g \end{cases} \tag{5}$$

Where subscripts l and g refer to liquid and gas.

Motion equations

Solver naoe-FOAM-SJTU contains a 6-degrees-of-freedom module which can solve the motion response of platform in all six motion degrees. Two coordinate systems are introduced

to describe the motion pattern of structures: a global coordinate system for calculating forces and defining movements, and a local coordinate system for constructing motion equations. The 6-degrees-of-freedom equations can be established with respect to the local coordinate system [7]:

$$\begin{cases} \dot{u} = X/m + vr - wq + x_g(q^2 + r^2) - y_g(pq - \dot{r}) - z_g(pr + \dot{q}) \\ \dot{v} = Y/m + wp - ur + y_g(r^2 + p^2) - z_g(qr - \dot{p}) - x_g(qp + \dot{r}) \\ \dot{w} = Z/m + uq - vp + z_g(p^2 + q^2) - x_g(rp - \dot{q}) - y_g(rp + \dot{p}) \\ \dot{p} = \frac{1}{I_x}\left\{K - (I_z - I_y)qr - m[y_g(\dot{w} - uq + vp) - z_g(\dot{v} - wp + ur)]\right\} \\ \dot{q} = \frac{1}{I_y}\left\{M - (I_x - I_z)rp - m[z_g(\dot{u} - vr + wq) - x_g(\dot{w} - uq + vp)]\right\} \\ \dot{r} = \frac{1}{I_z}\left\{N - (I_y - I_x)pq - m[x_g(\dot{v} - wp + ur) - y_g(\dot{u} - vr + wq)]\right\} \end{cases} \quad (6)$$

Where m is the mass of the structure; I_x, I_y and I_z are moments of inertia around three axes of the local coordinate system; μ, v and ω are three components of translational velocity vector; p, q and r represent angular velocity vector ;x_g, y_g and z_g are the coordinates of center of gravity; X , Y , Z , K , M and N represent the forces and moments, which is the combination of sea loads and mooring loads, and can be transformed to local coordinate system from its global counterpart.

COMPUTATIONAL MODEL

Two semi-submersible platforms are concerned in this study. Parameters of these platforms and mooring systems are presented below.

Parameters of platform 1

Platform 1 mainly consists of three parts as shown in Figure 1: a deck, six columns and three pontoons. This platform is symmetric with respect to both longitudinal and transverse sections at centre plane. The primary parameters of platform 1 are listed in Table 1. And the arrangement of its mooring system is illustrated in Figure 2. Mooring lines are made up of 3 parts. Parameters of the mooring lines are listed in Table 2. A rectangular numerical tank is used as the computational domain, whose dimensions are Length[-75m,75m] × Width[-75m,75m]×Hight[-50m,20m], and it is illustrated in Figure 3. Platform 1 is located at (0, 0, 0) in this computational domain. Waves of two different period is studied in this paper, and their parameters are listed in Table 3. Incident waves in the sea are simplified to regular waves in this paper. According to a statistical material [8], the period of wave in the South China Sea varies from 5s to 6.5s. So 6s is chosen as the period of wave 1, and 5s is chosen as the period of wave 2.

Table 1 Primary parameters of platform 1

Primary parameters	Original	Case-I
Deck	m	50×25×3.3
Bottom of deck above baseline	m	9.7
Column	m	7.5×5×6.2
Longitudinal distance between centerlines of columns	m	20
Transverse distance between centerlines of columns	m	17.5
Pontoon	m	25×10×3.5
Distance between centerlines of pontoons	m	20
Tonnage	t	2970
Center of gravity above baseline	m	6.01
Pitch gyration radius	m	8.79

Table 2 Main properties of a multi-component mooring line

Position	Upper	Middle	Lower
Length(m)	80	400	180
Diameter(mm)	140	130	140
Young's Modulus (Pa)	1.0978e+11	9.7941e+10	1.0978e+11
Weight in Water (N/m)	981	67.73	981

Table 3 Wave parameters

Wave number	Wave 1	Wave 2
Length(m)	56.2056	39.0327
Period(s)	6	5
Amplitude(m)	1.5	1.5

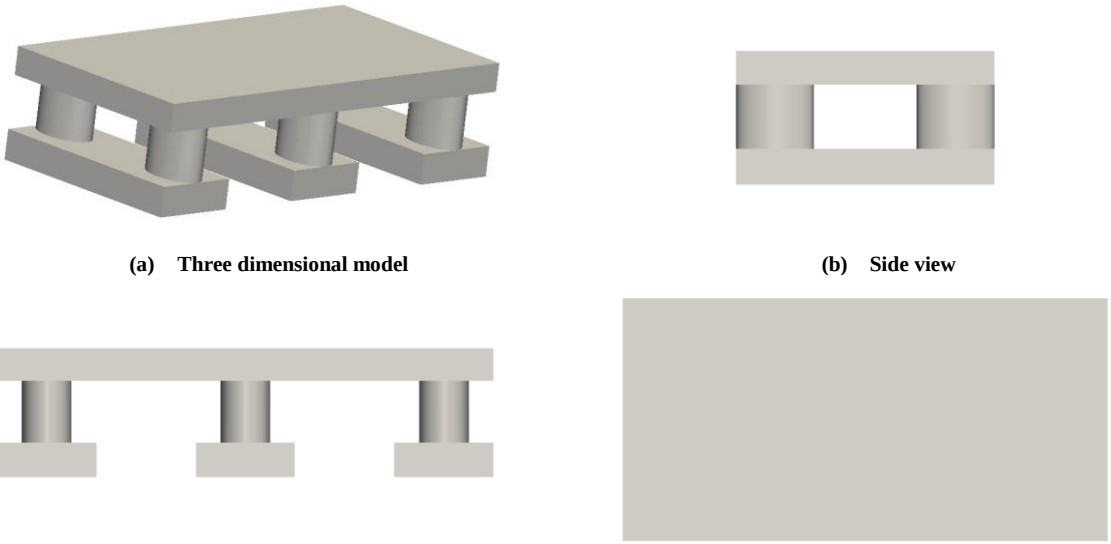

(a) Three dimensional model (b) Side view

(c) Front view (d) Top view

Fig. 1 Sketch of platform 1

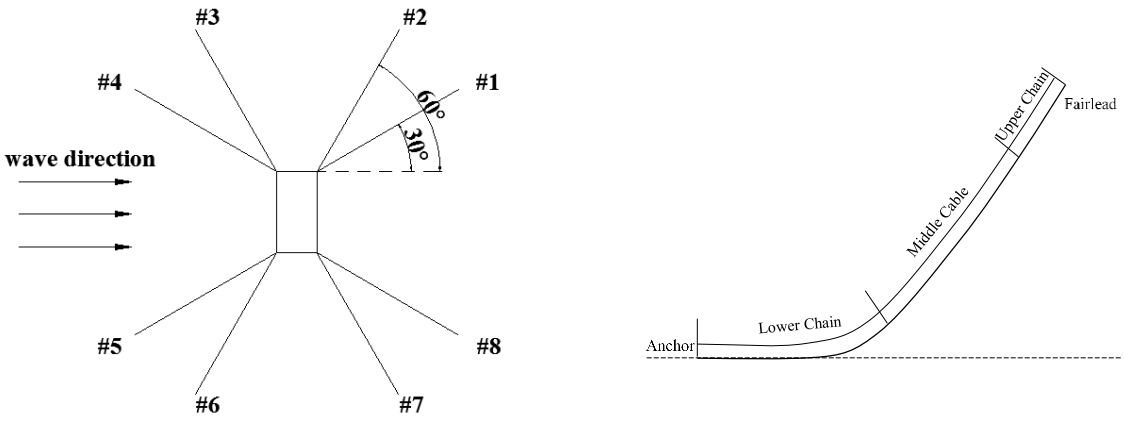

(a) Top view (b) Composition of a mooring line

Fig. 2 Arrangement of mooring system for platform 1

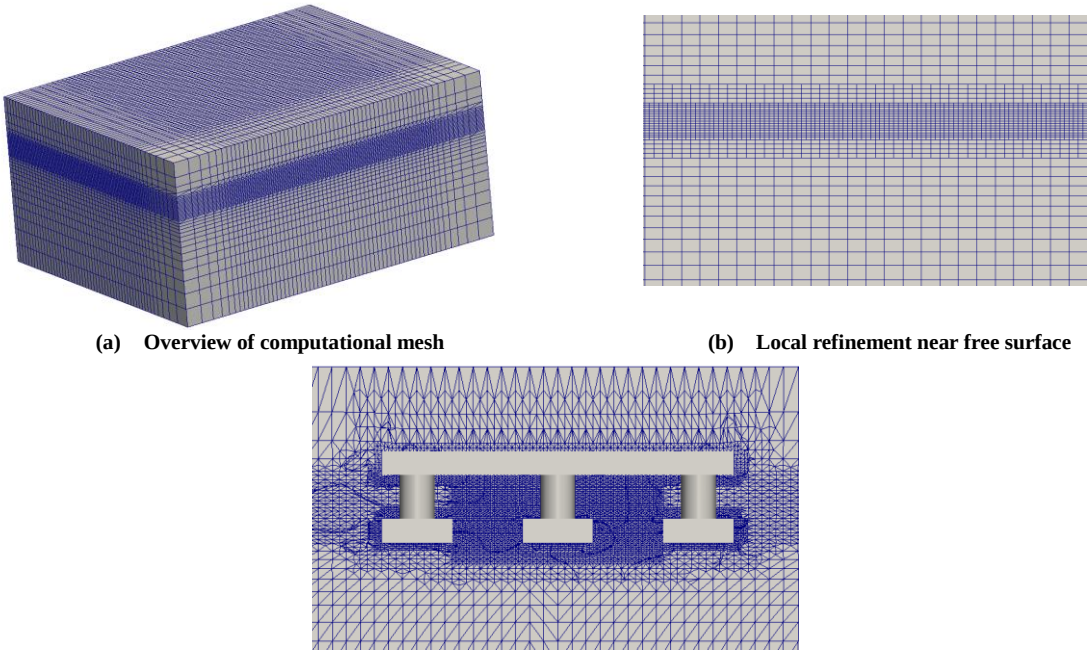

(a) Overview of computational mesh

(b) Local refinement near free surface

(c) Local refinement near the platform

Fig. 3 Global and local view of computational mesh

Parameters of platform 2

Platform 2, just like platform 1, mainly consists of three parts as shown in Figure 4: a deck, six cuboid pillars and three pontoons. This platform is symmetric with respect to both longitudinal and transverse sections at centre plane. The primary parameters of platform 1 are listed in Table 4. And the arrangement of mooring system is illustrated in Figure 5. Parameters of the mooring lines are the same as those of platform 1, which are listed in Table 2. And the computational domain is also the same as that of platform 1. Platform 2 is located at (0, 0, 0) in its computational domain. It is important to point out that, different from platform 1, the longer edges of platform 2 are parallel to the wave direction.

Table 4 Primary parameters of platform 2

Primary parameters	Original	Case-I
Deck	m	50×20×3
Bottom of deck above baseline	m	9
Cuboid pillar	m	10×4.5×5.5
Longitudinal distance between centerlines of columns	m	20
Transverse distance between centerlines of columns	m	9.5
Pontoon	m	20×10×3.5
Distance between centerlines of pontoons	m	20
Tonnage	t	2259
Center of gravity above baseline	m	6.75
Pitch gyration radius	m	51.32

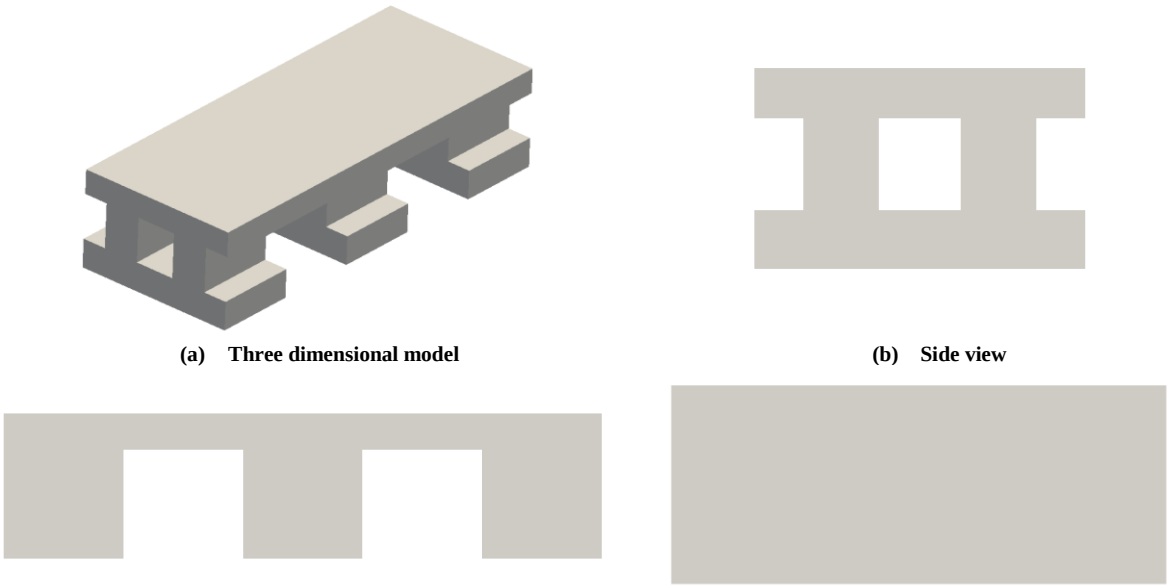

(a) Three dimensional model (b) Side view

(c) Front view (d) Top view

Fig. 4 Sketch of platform 2

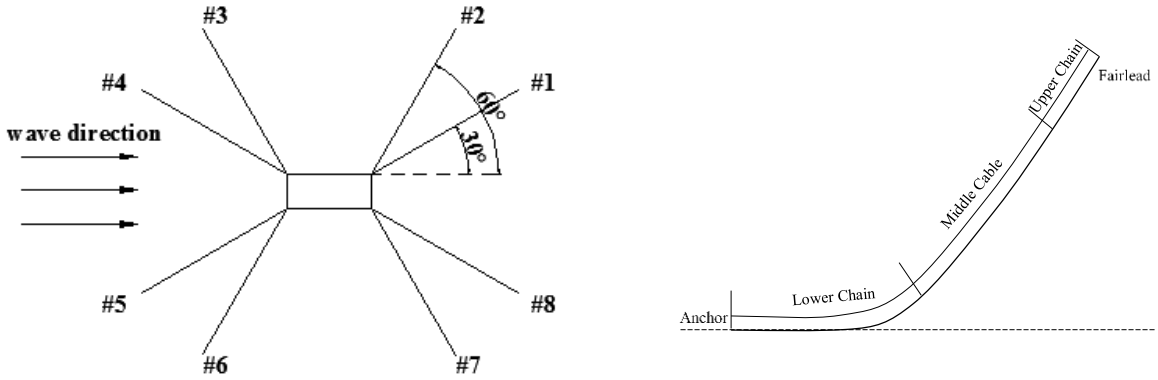

(c) Top view (d) Composition of a mooring line

Fig. 5 Arrangement of mooring system for platform 2

NUMERICAL RESULTS

Motion response of platform 1 in Wave 1

Incident wave propagates in longitudinal direction of the platform, and as is mentioned before, both platform 1 and platform 2 are symmetric with their own longitudinal sections at the centre plane. So only three degrees of freedom are considered, i.e. surge, heave and pitch.
Figure 6, Figure 7 and Figure 8 show surge, heave and pitch responses of platform 1. The result shows that the amplitude of surge comes near 1m when platform 1 works in wave 1. And the amplitude of heave is about 0.65m. The amplitude of pitch is about 0.75 degree. Platform 1 moves at the same period of incident wave.

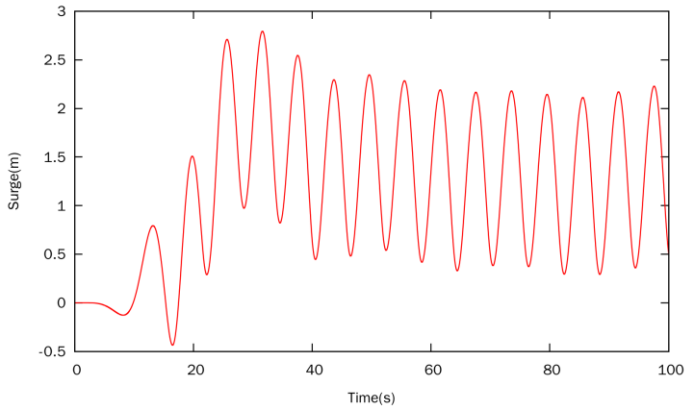

Fig. 6 Result of surge response for platform 1

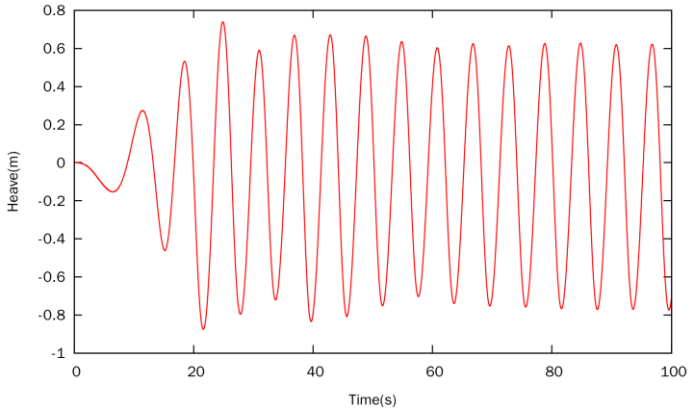

Fig. 7 Result of heave response for platform 1

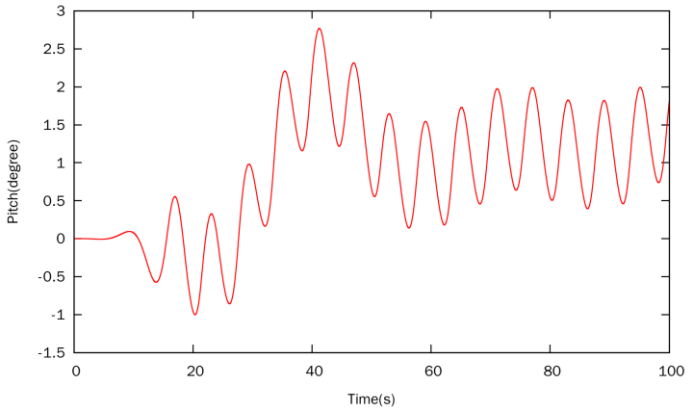

Fig. 8 Result of pitch response for platform 1

Figure 9 shows the tension of mooring line #1, #2, #3 and #4. And as is stated before, mooring line #1, #2, #3, and #4 are symmetrical to #8, #7, #6 and #5, so they have the same result with their corresponding mooring lines. It is indicated in this figure that the tension of #3 and #4 is larger than their initial pretension most of the time. On the contrary, tension of #1 and #2 is smaller than their initial pretension most of the time. The reason is that the average wave force tend to stretch #3 and #4, whereas the average wave force tend to release #1 and #2. Therefore, mooring line #3 and #4 provide the main resistance force to keep platform 1 near its initial position. In fact, the tension of mooring lines varies corresponding to the motion of platform 1. When platform 1 moves along the wave direction, tension in #3 and #4 increases, and tension in #1 and #2 decreases. When it comes to #3 and #4, #4 bears larger

tension than #3, and this is because the component of #4 in wave direction is larger than that of #3.

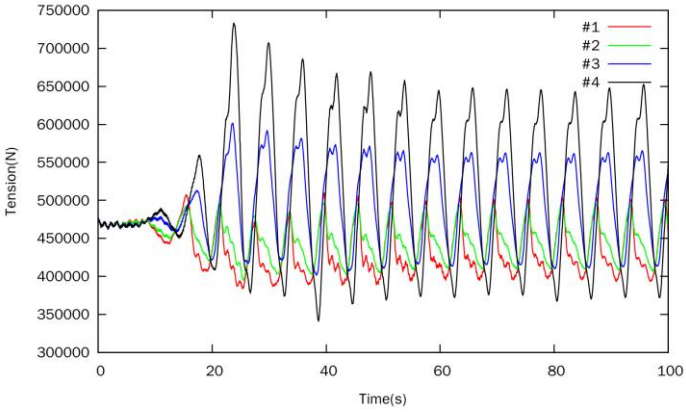

Fig. 9 Result of mooring-line force for platform 1

Comparison of the motion responses (platform 1) in Wave 1 and Wave 2

In this chapter, the motion responses of platform 1 affected by different waves are compared. Figure 10 shows the surge of platform 1 working in wave 1 and wave 2. It indicates that the amplitude of surge response decreases when the incident wave changes from wave 1 to wave 2, and both the two incident waves make platform 1 experience a drift along the wave direction.

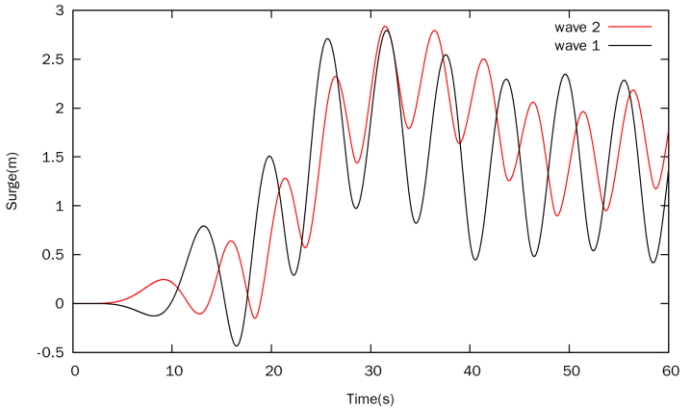

Fig. 10 Comparison of surge for platform 1 and 2

Figure 11 shows the heave of platform 1 working in wave 1 and wave 2. It indicates that the amplitude of heave response decreases when the incident wave changes from wave 1 to wave 2.

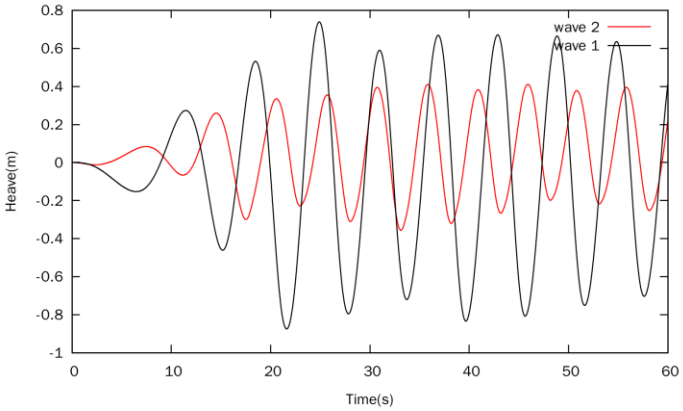

Fig. 11 Comparison of heave for platform 1 and 2

Figure 12 shows the pitch of platform 1 when it works in wave 1 and wave 2. It indicates that platform 1 slightly inclines towards the direction of wave most of the time.

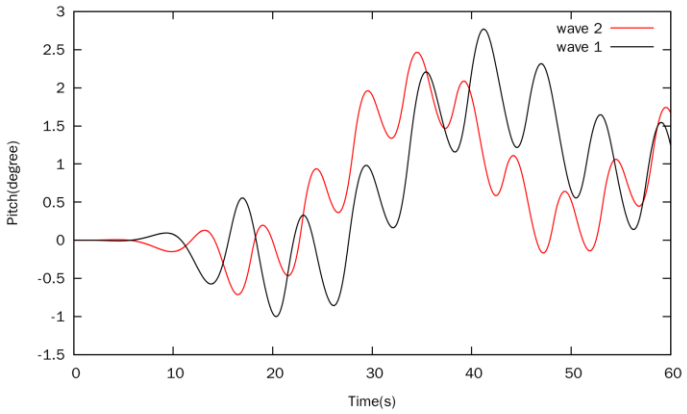

Fig. 12 Comparison of pitch for platform 1 and 2

Figure 13 shows that, just like result in the previous chapter, the tension of #3 and #4 is larger than their initial pretension most of the time. On the contrary, the tension of #1 and #2 is smaller than their initial pretension most of the time.

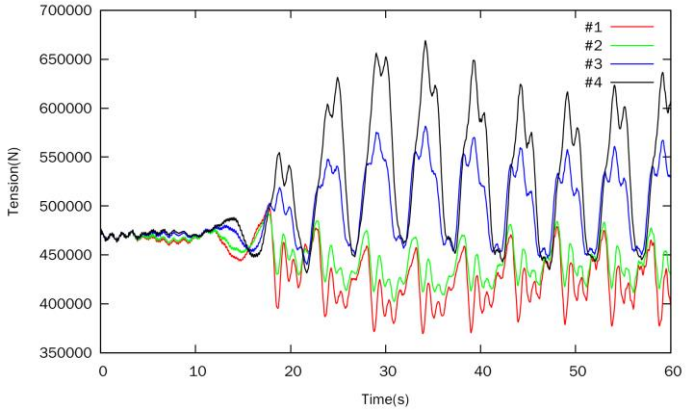

Fig. 13 Result of mooring-line force for platform 1

Motion response of platform 2 in Wave 1

Figure 14, Figure 15 and Figure 16 show surge, heave and pitch responses of platform 2. The result shows that the amplitude of surge comes near 0.3m when platform 2 work in wave 1. And the amplitude of heave is about 0.2m, the amplitude of pitch is about 0.75 degree. Platform 2 moves at the same period of incident wave. And different with platform 1, the pitch of platform 2 varies around its initial position instead of having an incline towards wave direction. The fact that the pitch gyration radius, which provides most of the restoring moment, of platform 2 is much larger than that of platform 1 is the main reason which causes the difference.

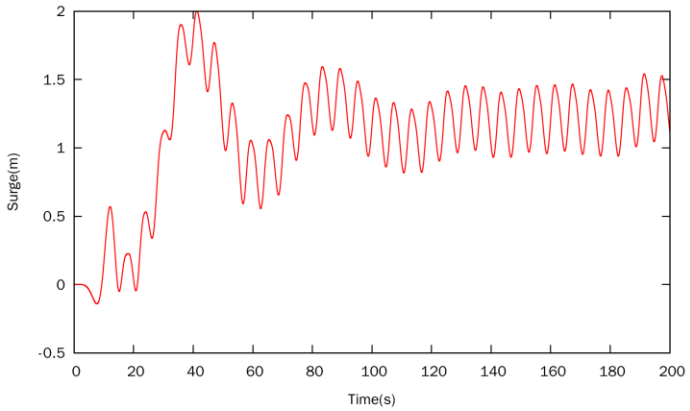

Fig. 14 Result of surge response for platform 2

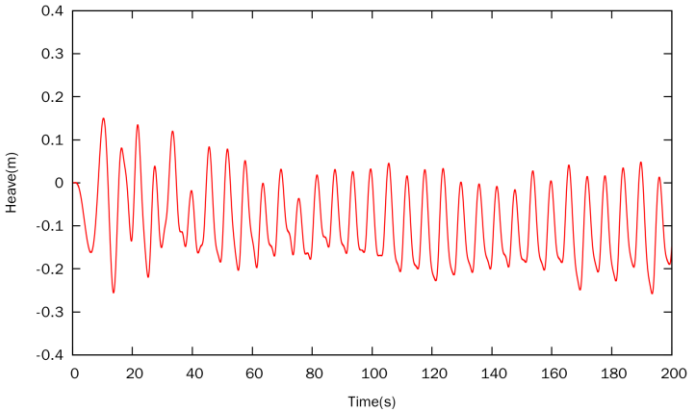

Fig. 15 Result of heave response for platform 2

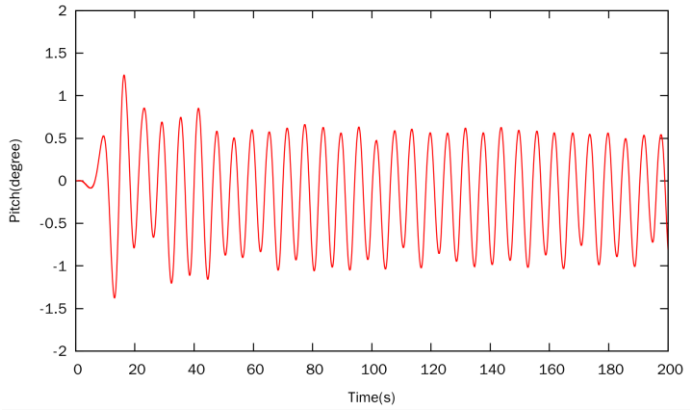

Fig. 16 Result of pitch response for platform 2

Figure 17 shows the tension of mooring line #1, #2, #3 and #4. Just like the result of platform 1, #3 and #4 bears larger tension than #1 and #2, and #4 bears larger tension than #3.

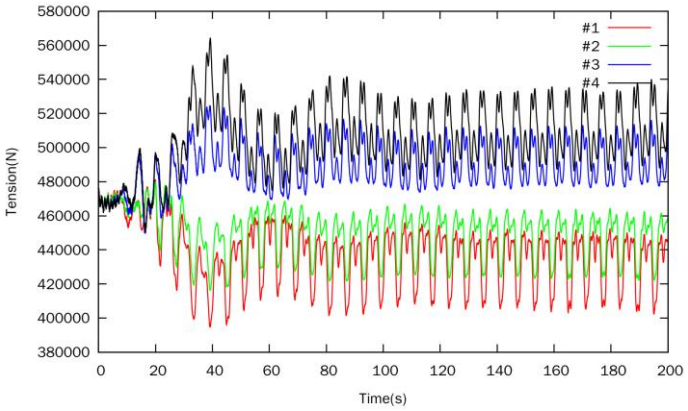

Fig. 17 Result of mooring-line force for platform 2

CONCLUSIONS

1. In terms of surge response, both of platform 1 and platform 2 have small drift along the incident-wave direction. The amplitude of surge response decreases when the incident wave of platform 1 changes from wave 1 (wave period is 6s) to wave 2 (wave period is 5s).
2. The amplitude of heave response decreases when the incident wave of platform 1 changes from wave 1 to wave 2. Both of the platforms move around the initial position in heave direction.
3. In terms of pitch response, platform 1 slightly inclines towards the direction of wave most of the time, while platform 2 moves around its initial position. The main reason of this difference is that the pitch gyration radius of platform 2 is much larger than that of platform 1.
4. The tension of #3 and #4 is larger than their initial pretension most of the time. On the contrary, tension of #1 and #2 is smaller than their initial pretension most of the time. Further more, #4 bears larger tension than #3.
5. Furhter work will focus on extreme sea conditions and shallow water conditions. And we can use naoe-FOAM-SJTU to generate irregular waves, thus simulating more complex sea conditions.

ACKNOWLEDGEMENTS

This work is supported by the National Natural Science Foundation of China (51379125, 51490675, 11432009, 51579145, 11272120), Chang Jiang Scholars Program (T2014099), Program for Professor of Special Appointment (Eastern Scholar) at Shanghai Institutions of Higher Learning (2013022), and Innovative Special Project of Numerical Tank of Ministry of Industry and Information Technology of China (2016-23/09), to which the authors are most grateful.

REFERENCES

1. Tahar, A., Kim, M.H. (2008) Coupled-dynamic analysis of floating structures with polyester mooring lines[J]. Ocean Engineering. **35**: 1676-1685.
2. Kim, B.W., Sung, H.G., Kim, J.H., Hong, S.Y. (2013) Comparison of linear spring and nonlinear FEM methods in dynamic coupled analysis of floating structure and mooring system[J]. Journal of Fluids and Structures. **42**: 205-227.
3. Sethuraman, L., Venugopal, V. (2013) Hydrodynamic response of a stepped-spar floating wind turbine: Numerical modelling and tank testing[J]. Renewable Energy. **52**: 160-174.
4. Yilmaz, O., Incecik, A. Hydrodynamic design of moored floating platforms [J]. (1996) Marine Structures. **9**(5): 545-575.
5. Carlos Lopez-Pavon, Rafael A. Watai, Felipe Ruggeri, Alexandre N. Simos. (2013) Influence of wave induced second-order forces in semi-submersible FOWT mooring design. Conf. on Ocean, Offshore and Arctic Engineering, France.
6. Hirt, C.W., Nichols, B.D. (1981) Volume of fluid (VOF) method for the dynamics of free boundaries [J]. Journal of Computational Physics. 39(1): 201-225.
7. Liu, Y., Peng, Y., Wan, D.C. (2015) Numerical investigation on interaction between a semi-submersible platform and its mooring system. Conf. on Ocean, Offshore and Arctic Engineering, Canada.
8. Zheng. C, Li. X, Sun. C. (2014) Meticulous simulation of seasonal characteristics of the China sea wave period. Advances in Marine Sciences, 2014,1, 44-49.
9. Shen, Z., Cao, H., Ye, H., Liu, Y., Wan, D.C. (2013) Development of CFD Solver for Ship and Ocean Engineering Flows. In 8th International OpenFOAM Workshop. Jeju, Korea.
10. Shen, Z., Wan, D.C. (2012) Numerical Simulations of Large-Amplitude Motions of KVLCC2 with Tank Liquid Sloshing in Waves. In 2nd International Conference on Violent Flows. Nantes, France. 2012: 149-156.
11. Shen, Z., Wan, D.C. (2013) RANS Computations of Added Resistance and Motions of a Ship in Head Waves [J]. International Journal of Offshore and Polar Engineering. **23**(4): 263-271.
12. Cao, H., Liu, Y., Wan, D.C., Yang, C. (2011) Numerical simulation of solitary wave impact on fixed offshore platform. In The 7th International Workshop on Ship Hydrodynamics. Shanghai, China. 2011a: 138-143.
13. Cao, H., Wan, D.C. (2014) Development of Multidirectional Nonlinear Numerical Wave Tank by naoe-FOAM-SJTU Solver [J]. International Journal of Ocean System Engineering. **4**(1): 52-59.
14. Cao, H., Wang, X., Liu, Y., Wan, D.C. (2013) Numerical Prediction of Wave Loading on a Floating Platform Coupled with a Mooring System. In The Twenty-third International Offshore and Polar Engineering Conference. Anchorage, Alaska, USA. 2013: 582-589.
15. Cao, H., Zha, J., Wan, D.C. (2011) Numerical simulation of wave run-up around a vertical cylinder. In Proceedings of the Twenty-first (2011) International Offshore and Polar Engineering Conference, Maui, Hawaii, USA. 2011b: 726-733.